

Flexible Free-standing PEDOT:PSS/MnO₂ Films as Electrode Material for Supercapacitors

Xuejing Li^{1,2}, Chen Zhou³, Lanlan Shen³, Weiqiang Zhou¹, Jingkun Xu^{1,*}, Chan Luo³, Jian Hou², Rongri Tan^{3,*} and Fengxing Jiang^{3,*}

¹ College of Pharmacy, Jiangxi Science and Technology Normal University, Nanchang 330013, P. R. China

² State Key Laboratory for Marine Corrosion and Protection, Luoyang Ship Material Research Institute, Qingdao 266101, P. R. China

³ Jiangxi Key Laboratory of functional organic molecules, Jiangxi Science and Technology Normal University, Nanchang 330013, P. R. China

Corresponding authors. Fax: +86-791-83823320, Tel.: +86-791-88537967

*E-mail: xujingkun1971@yeah.net (J. Xu); rrtan@163.com (R. Tan); f.x.jiang@live.cn (F. Jiang)

Received: 3 August 2018 / *Accepted:* 28 September 2018 / *Published:* 10 April 2019

A free-standing and flexible film is desired for wearable energy devices in the future. MnO₂ has attracted wide interest as a promising electrode material for high energy density supercapacitors. However, it suffers from the poor electron transfer and film-forming properties. On the contrary, the excellent conducting polymer poly(3,4-ethylenedioxythiophene):poly(styrene sulfonate) (PEDOT:PSS) has a high electrical conductivity with poor specific capacitance. Herein, we designed and fabricated a composite film by combining PEDOT:PSS and MnO₂ nanoparticles (NPs) via a facile dilution-filtration. MnO₂ NPs were prepared by a simple and environmental friendly method. PEDOT:PSS plays a significant role on the formation of free-standing and flexible composite film. Meanwhile, it enhances the electron transfer property of MnO₂ NPs due to the high electrical conductivity of PEDOT:PSS. The as-prepared PEDOT:PSS/MnO₂ composite films show enhanced electrochemical performance and specific capacitance, which is three times higher than PEDOT:PSS films. This facile composite method provide a potential application in future flexible supercapacitor.

Keywords: Free-standing films; flexible supercapacitor; PEDOT:PSS; MnO₂

1. INTRODUCTION

Nowadays, as the increase of energy demand, the development of energy storage devices is gaining more and more interest owing to over use of fossil fuels.[1, 2] Supercapacitor has been regarded as one of the most promising candidates for energy storage devices. It has attracted significant interest

because of high power density, fast charging-discharging processes, long cycle life, and environmental friendliness.[3-5] Pseudocapacitors (PCs) based on redox reaction (Faradaic reactions) between electrode materials including metal oxides and conducting polymers and electrolyte have the desirable properties during fast and reversible redox that enables the enhancement of charge storage.[2, 3, 6]

Conducting polymers have attracted extensive attention in flexible electronic devices,[7] due to their apparent features in light weight and excellent mechanical flexibility. Such advantages are urgently required with ever-increasing development of portable and wearable electronics.[8-10] Among conducting polymers, poly(3,4-ethylenedioxythiophene):poly(styrene sulfonate) (PEDOT:PSS) with the good film-forming feature is a good candidate for energy storage materials. It also can promote electron transport in composites and improve the capacitance property.[11-13] Currently, many composite thin films showed poor free-standing property as flexible supercapacitors, such as PEDOT:PSS/MnO₂,[14] CNT/PEDOT:PSS,[15] and RuO₂/PEDOT:PSS[16], which are limited by the traditional film-forming methods of PEDOT:PSS. Generally, PEDOT:PSS thin films obtained by common coating and dipping on flexible substrates easily led to the poor electron transport property. Without support of substrates, flexible free-standing films directly used as electrode have drawn great attention.[9, 17] Dilution-filtration has been confirmed to be an efficient method to prepare flexible free-standing PEDOT:PSS films with large area and tunable film thickness.[18] More importantly, its electrical conductivity can be improved over 1000 S cm⁻¹ by removing resident PSS with organic solvents. Although a high electron transport property for PEDOT:PSS can be completed by a facile dilution-filtration, it still suffers from a low specific capacitance.[19, 20]

Transition metal oxides have acquired great attention as electrode materials for supercapacitors owing to their high theoretical specific capacitance and good chemical stability, such as ZnO, Fe₃O₄, Co₃O₄, MnO₂, RuO₂, and SnO₂ [21-24] in recent years. Among them, MnO₂ has been recognized as one of the most promising electrode materials due to its low-cost, natural abundance, good electrochemical properties, and high theoretical capacitance value.[6, 23, 25] However, it suffers from low specific surface area, low electrical conductivity (10⁻⁵-10⁻⁶ S cm⁻¹), and low electron transfer efficiency, thus resulting in huge difference between practical and theoretical values.[26, 27] Moreover, the fine grain state of MnO₂ NPs hinders its good film-forming property. Therefore, it is vital for supercapacitor materials to improve the electrical conductivity and the film-forming of MnO₂ NPs. Currently, one of the most effective methods is to prepare composite by combining different materials with the good electron transfer efficiency and high specific capacitance. Conducting polymer is a promising candidate in improving the specific capacitance and the film-forming property of MnO₂.

Composite thin films based on PEDOT:PSS and MnO₂ NPs are considered as attractive rechargeable electrode materials for electrochemical energy storage.[12] In this work, the α -MnO₂ NPs were successfully prepared by sequential redox and annealing treatment. PEDOT:PSS plays an important role in achievement of good flexible composite thin film with MnO₂ NPs. A free-standing PEDOT:PSS/MnO₂ composite film was successfully prepared through a simple vacuum filtration. PEDOT:PSS/MnO₂ films were systematically investigated as flexible supercapacitor.

2. EXPERIMENTAL DETAILS

2.1. Chemicals

PEDOT:PSS aqueous solution (Clevios PH1000), ethanol (EtOH; 99.8 %; chromatographically pure; J&K Scientific Co. Ltd), potassium permanganate (KMnO₄; 99.9%; analytical grade; Xilong Scientific), sodium sulfite (J&K Scientific Co. Ltd), and polyvinylidene fluoride (PVDF) membrane (pore size: 0.45 mm; J&K Scientific Co. Ltd) were used directly as received.

2.2. Preparation

A 50 mM of KMnO₄ solution was prepared by dissolving KMnO₄ in distilled water, and 35 mL of ethanol was added into 20 mL of KMnO₄ solution by stirring. The resultant solid precipitates were washed with distilled water and ethanol until neutral pH value, then dried at 60 °C for 12 h. Finally, the resultant productions were annealed at 400 °C in tube furnace for 3 h. Various contents MnO₂ NPs after annealing were mixed with the 20, 40, 50, and 60 wt.% PEDOT:PSS in EtOH. Finally, the flexible free-standing PEDOT:PSS/MnO₂ composite films were fabricated by direct filtration and dried at 60 °C for 2 h.

2.3. Characterization

The structural and compositional information were characterized by X-ray powder diffraction (XRD: D8 Advance instrument), transmission electron microscopy (TEM: Tecnai-G20 microscope), scanning electron microscopy (SEM: QUANTA Q400), and X-ray photoelectron spectroscopy (XPS: SCALAB 250Xi). An electrochemical workstation (CHI660E: Shanghai CH Instruments Co., China) was used to execute the cyclic voltammetry (CV) and galvanostatic charge-discharge (GCD). A Pt plate/composite film, graphite and glassy carbon electrode (SCE) were used as the working electrode, counter electrode, and reference electrode, respectively. Potential range of 0.0-0.9 V was applied for CV and GCD measurements. A 0.5 M Na₂SO₄ was used as electrolyte.

3. RESULTS AND DISCUSSION

The scheme for the fabrication of PEDOT:PSS/MnO₂ composite thin films is illustrated in Figure 1a. MnO₂ NPs were synthesized by dropping EtOH into KMnO₄ solution and annealed at 400 °C in vacuum tube furnace for 3 h. The impurity on MnO₂ NPs can be removed by high temperature annealing.[28, 29] The as-annealed MnO₂ NPs were re-dispersed into EtOH by ultrasonic cell disruptor. The composite thin films of PEDOT:PSS/MnO₂ were fabricated by dispersing various mass of MnO₂ in PEDOT:PSS solution, and diluted to be 5 mL of EtOH solution. As we know, it is difficult for MnO₂ NPs to form high-quality free-standing films. However, PEDOT:PSS with an excellent film-forming property allows the proper contents of MnO₂ NPs to implant into the PEDOT:PSS matrix and eventually

obtain a good free-standing film. As shown in Figure 1b, the as-prepared PEDOT:PSS/MnO₂ show the free-standing composite thin films with good flexibility. The free-standing property apparently decreases since no enough PEDOT:PSS are used to interconnect and form a good film in the case that the MnO₂ NPs contents are more than 50 wt.%. The free-standing thin films are desired to enable a better electron transport property and develop the flexible wearable electron devices.

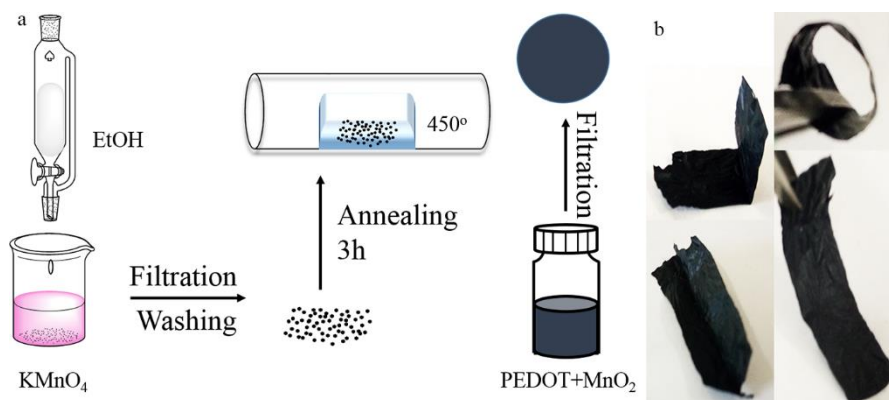


Figure 1. Schematic fabrication (a) and digital photos (b) of the flexible free-standing PEDOT:PSS/MnO₂ composite thin films.

Figure 2a illustrates the powder XRD pattern of as-prepared MnO₂ NPs. The diffraction peaks at $2\theta = 18.1^\circ, 28.8^\circ, 37.5^\circ$ and 49.9° are assigned to the plane (200), (310), (211) and (411), respectively, which are well consistent with the predominate α -MnO₂ (JCPDS No. 44-0141).[30, 31] Figure 2b and 2c show the TEM images of MnO₂ NPs with different magnification. One can obviously see that the as-prepared MnO₂ NPs exhibit the homogeneous grain structure and have the length ranging from 50 to 70 nm. Additionally, the interplanar spacing of the (211) and (411) planes are 0.21 and 0.26 nm, respectively, further confirming the successful synthesis of α -MnO₂ NPs, as shown in the high-magnification TEM image of Figure 2d.

SEM images of pure PEDOT:PSS and PEDOT:PSS/MnO₂ composite samples are presented in Figure 3. The PEDOT:PSS film presents the homogeneous and smooth surface, as shown in Figure 3a. This suggests that the pure PEDOT:PSS film prepared by EtOH dilution-filtration has the good film-forming property. It also can be believed that the PEDOT:PSS/MnO₂ composite film with proper MnO₂ NPs can complete a free-standing film. Figure 3b shows the SEM image of PEDOT:PSS/MnO₂ composite film with 50 wt.% MnO₂ NPs. Obviously, it can be found that the as-prepared MnO₂ NPs are well-dispersed in PEDOT:PSS network and wrapped by PEDOT:PSS. Although the surface of PEDOT:PSS/MnO₂ become more rough compared to pure PEDOT:PSS film, the as-prepared composite films still keep good free-standing shape observed in Figure 1b. It also implies that the electron transport property of MnO₂ NPs is likely to be improved by the PEDOT:PSS. It is worth mentioning that the poor free-standing property of composite thin films can be observed apparently as the increase of MnO₂ content more than 50 wt.%. This inevitably impacts the electron transport property of PEDOT:PSS/MnO₂ with respect to its flexibility and film-forming property.

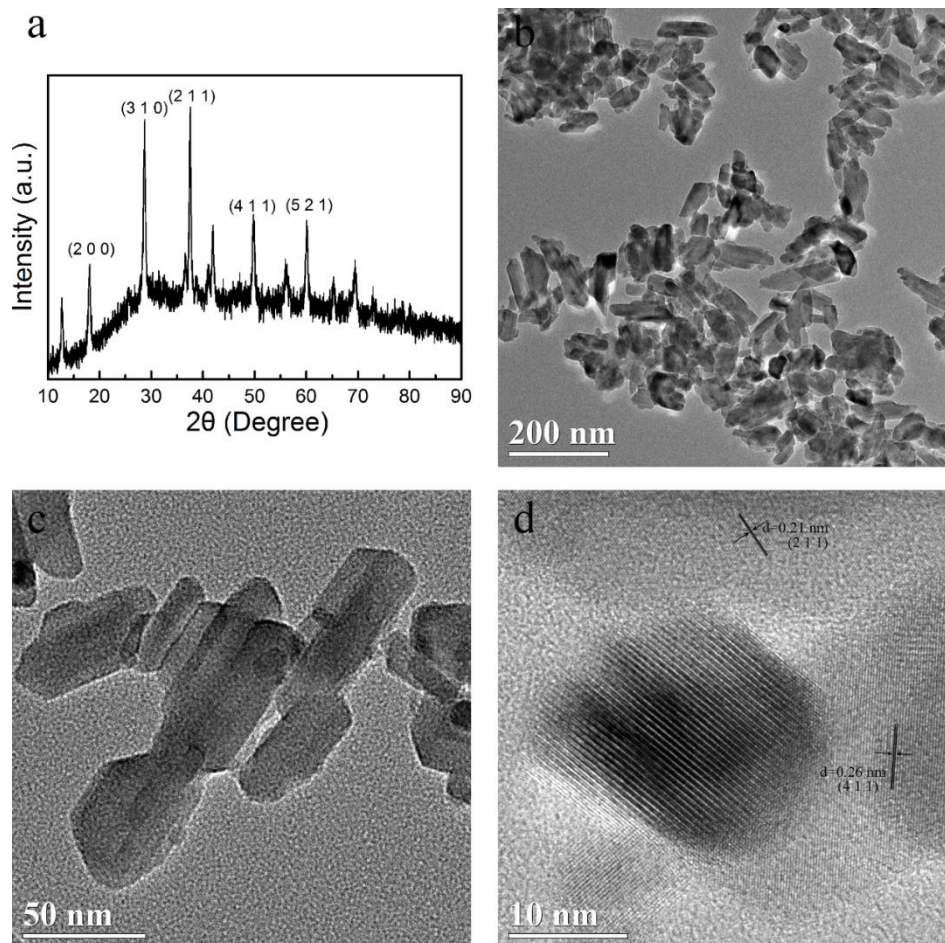


Figure 2. XRD patterns (a), TEM images of various magnification (b and c) and high-magnification TEM image (d) of the as-prepared MnO₂ NPs.

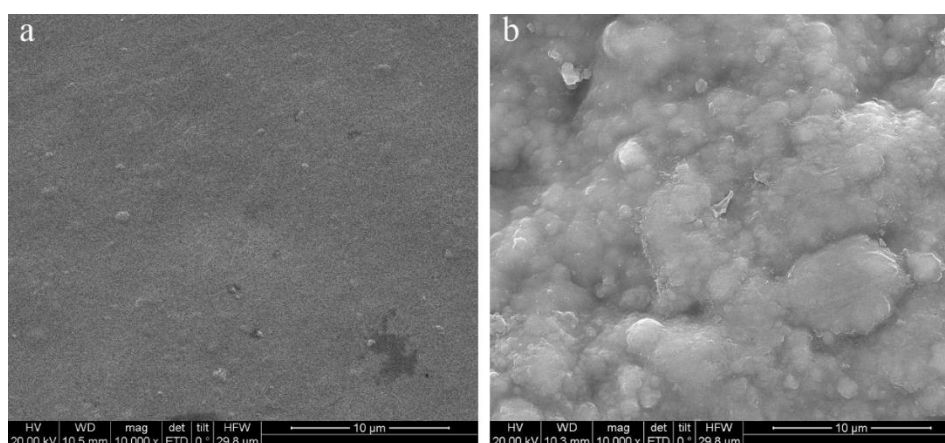


Figure 3. SEM images of PEDOT:PSS (a) and PEDOT:PSS/MnO₂ with 50 wt.% MnO₂ (b) composite films.

The X-ray photoelectric spectroscopy (XPS) was further employed to investigate the composition of PEDOT:PSS/MnO₂ composite films with 50 wt.% MnO₂ NPs. As shown in Figure 4a, the XPS spectra shows the S_{2p} for the pure PEDOT:PSS (red curve) and PEDOT:PSS/MnO₂ (blue curve).

The peaks between 166 and 172 eV correspond to the sulfur atoms from the sulphonate group in PSS, while the two peaks from 162 to 166 eV are relative to the sulfur atom from thiophene group in PEDOT.[32, 33] One can find that the ratio of PEDOT to PSS is 1:2.05 for the filtering PEDOT:PSS/MnO₂, which become larger compared with that of the pure film (1:3.34). The increased ratio of PEDOT to PSS indicates the dilution-filtration method can effectively remove partial PSS from PEDOT:PSS. The peaks at 654.16 eV and 642.31 eV in Figure 4b are assigned to the Mn 2p_{1/2} and Mn 2p_{3/2}²³ with a spin-energy separation of 11.8 eV similar to the previous reports for MnO₂ NPs,[6, 25, 34, 35] further confirming the successful preparation of MnO₂ NPs.

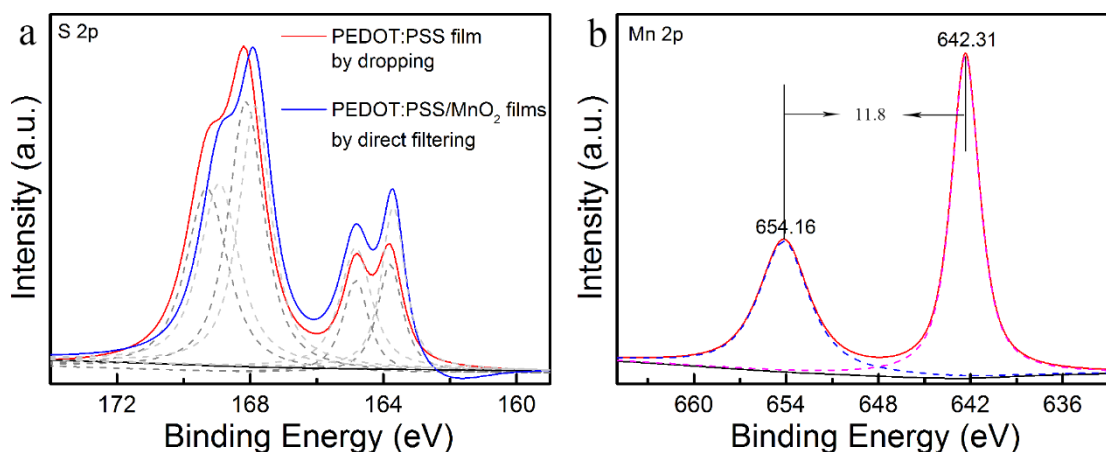


Figure 4. S 2p (a) from the pure PEDOT:PSS and PEDOT:PSS/MnO₂, and Mn 2p (b) XPS specific fitting of spectra for PEDOT:PSS/MnO₂ composite films with 50 wt.% MnO₂.

As we know, the pure PEDOT:PSS shows the poor electrical conductivity of 10⁻¹ S cm⁻¹, which is not good for the effective improvement of electron transport of MnO₂ NPs. Factually, it has been confirmed that the dilution-filtration with organic solvents can effectively enhance the electrical conductivity of PEDOT:PSS films (>1000 S cm⁻¹).[13, 18] In view of this, the MnO₂ NPs were dispersed in PEDOT:PSS EtOH solution, and the PEDOT:PSS/MnO₂ composite films were fabricated by one-step filtration. The electrical conductivity of PEDOT:PSS/MnO₂ composite film was increased to 17 S cm⁻¹, which is higher by two magnitudes than pure PEDOT:PSS. The removal of non-conductive PSS via dilution-filtration contributed to the enhancement of electrical conductivity, which can be confirmed in XPS (Figure 4a). Meanwhile, one can find that the electrical conductivity of composite films gradually decreases with the increasing MnO₂ NPs, which is due to the poor connecting network of PEDOT:PSS caused by the high content of MnO₂ NPs.

To take a flexible free-standing film with high electron transport into account, the contents of MnO₂ NPs in composite films were controlled less than 50 wt.% for the next electrochemical measurements. Moreover, controlling of MnO₂ NPs contents in PEDOT:PSS matrix is very important for optimizing specific capacitance of composite electrodes. To investigate the effect of MnO₂ NPs contents on the specific capacitance, GCD and CVs were performed to evaluate the electrochemical capacitive properties of PEDOT:PSS/MnO₂ composite films, as illustrated in Figure 5.

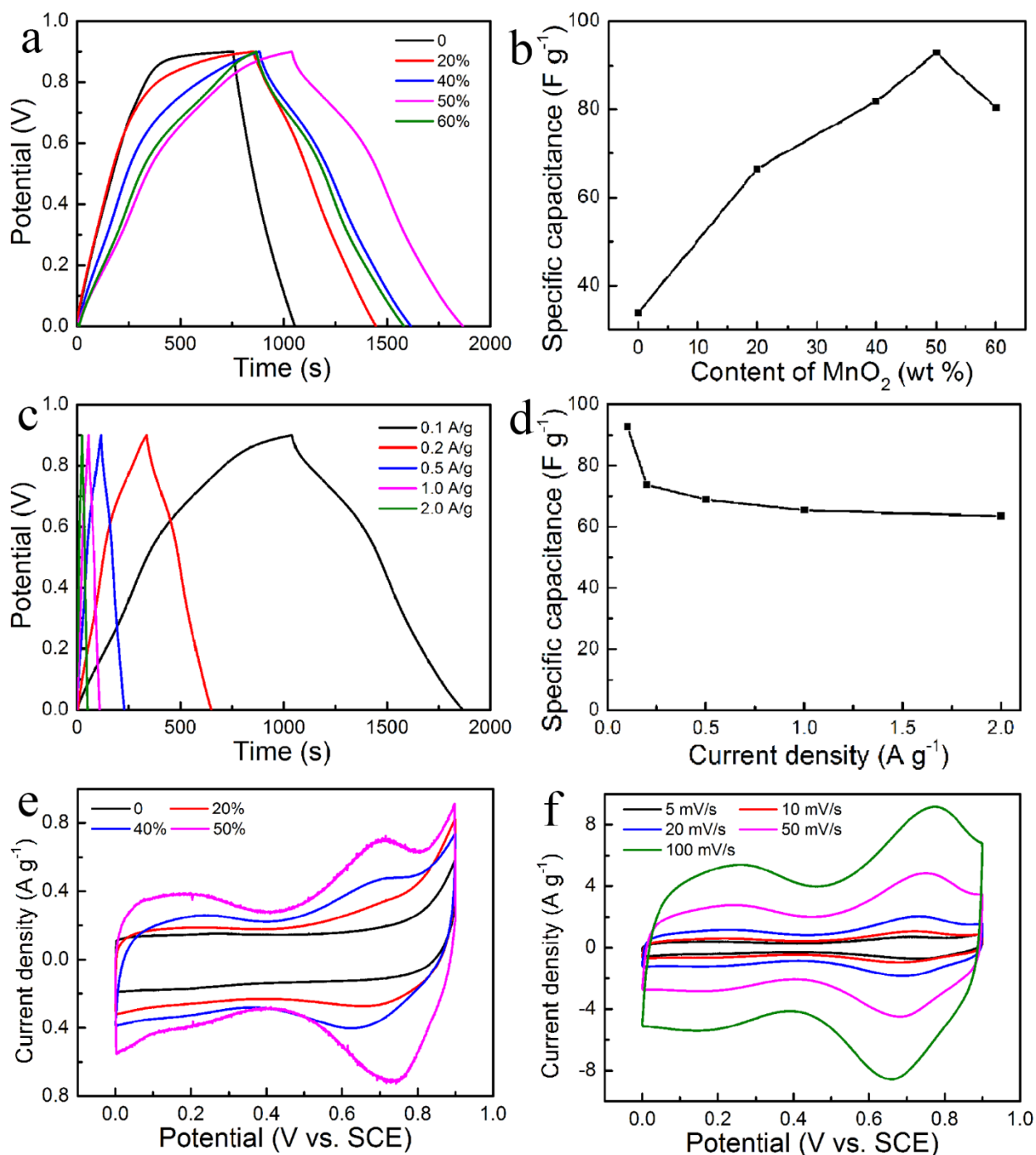


Figure 5. The GCD curve (a) and the specific capacitance (b) of PEDOT:PSS/MnO₂ with 0, 20, 40, 50, and 60 wt.% MnO₂ at the current density of 0.1 A g⁻¹. The GCD curves (c) and the specific capacitance (d) of PEDOT:PSS/MnO₂ with 50 wt.% MnO₂ at the current densities of 0.1, 0.2, 0.5, 1.0 and 2.0 A g⁻¹. (e) The CV curves of PEDOT:PSS/MnO₂ with the MnO₂ contents of 0, 20, 40, and 50 wt.% at a scan rates of 5 mV s⁻¹. (f) The CV curves of PEDOT:PSS/MnO₂ with 50 wt.% MnO₂ at a scan rate of 5, 10, 20, 50, and 100 mV s⁻¹.

The as-prepared free-standing PEDOT:PSS/MnO₂ composite films with various MnO₂ contents were directly employed as the working electrode for electrochemical measurements. The

electrochemical performance of supercapacitor were evaluated from the time constant of charge and discharge, symmetry, and resistance drop value of GCD curves.[36] The GCD curves reflecting specific capacitances of various samples are shown in Figure 5a-d. The capacitive properties of the as-synthesized MnO₂ were also investigated by GCD tests according to the equation of

$$C = \frac{It}{mV} \quad (1)$$

where C , I , and t are specific capacitance (F g⁻¹), the discharge current (A), and time (s), respectively. V and m are the potential range (V) and the mass of individual sample.

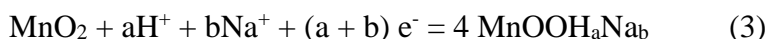
Figure 5a exhibits the GCD of composite electrodes with 0, 20, 40, 50, and 60 wt.% MnO₂ at 0.1 A g⁻¹. The GCD curves show the typical redox linear and symmetric triangular shapes. The calculated specific capacitances are recorded in Figure 5b. One can observe that the specific capacitance for the composite films increases as the increase of MnO₂ NPs contents. It can be found that the free-standing PEDOT:PSS/MnO₂ films with 50 wt.% MnO₂ NPs delivers the highest capacitance of 92.8 F g⁻¹, which is higher than pure PEDOT:PSS film (33.9 F g⁻¹ at 0.1 A g⁻¹). It indicates that the introduction of MnO₂ NPs presents a positive effect on the performance of pure conducting polymer film. The increase of capacitance for composite films (content of 20-50 wt.%) can be ascribed to the MnO₂ NPs, which prolongs the time constant of charge and discharge. The time of discharging become lower for the PEDOT:PSS/MnO₂ composite film containing 60 wt.% MnO₂ compared with that of 50 wt.%. It suggests that the excess MnO₂ NPs contents result in lower specific capacitance. This is due to the excessive MnO₂ in PEDOT:PSS leading to a bad conductive PEDOT network and the large increase of film resistance, which is related to its poor film-forming ability of the composite film.

Figure 5c exhibits the GCD results of the PEDOT:PSS/MnO₂ film electrode with 50 wt.% MnO₂ NPs. According to Figure 5c, the calculated specific capacitances of 92.8, 73.8, 68.9, 65.38, and 63.5 F g⁻¹ were obtained at the different current densities of 0.1, 0.2, 0.5, 1.0, and 2.0 A g⁻¹. One can see the specific capacitance reduces with the increase of current density, which is attributed to the practical diffusion conditions. Non-ideal condition led to the limited ions in electrolyte and the low efficiency of the active materials.[37] Noted that, there is no obvious voltage drop for the GCD curves in Figure 5a and 5c, indicating good reversible redox reaction. Figure 5e shows the CVs of pure and composite films with the MnO₂ contents ranging from 20 to 50 wt.% between 0 and 0.9 V at a scan rate of 5 mV s⁻¹. The performance of specific capacitance (C) were investigated by CVs according to the equation of

$$C = \frac{\int_{E_1}^{E_2} i(E)d(E)}{2vm(E_2-E_1)} \quad (2)$$

where E_1 and E_2 are the cut off potentials in CVs, respectively. $i(E)$, $\int i(E)d(E)$, and v are the instantaneous current, the voltammetry charge acquired by integrating the negative sweep in the CVs, and the scan rate. It can be found that the CV curves present the similar profile with different active area for the PEDOT:PSS/MnO₂ composite electrodes. The active area becomes larger than the pure PEDOT:PSS films after the introduction of MnO₂ NPs, which indicates that the MnO₂ NPs have positive influence on the enhancement of capacitance property for pure PEDOT:PSS films. Based on the CVs curves, the specific capacitance of PEDOT:PSS/MnO₂ with 50 wt.% MnO₂ was 87.4 F g⁻¹ which was about three times larger than that of pure PEDOT:PSS films (29.7 F g⁻¹) at a scan rate of 5 mV s⁻¹. Additionally, the PEDOT:PSS/MnO₂ film with 50 wt.% MnO₂ was further investigated by the CVs at the different scan rates of 5, 10, 20, 50, and 100 mV s⁻¹. According to the CVs in Figure. 5f, the calculated

specific capacitances of PEDOT:PSS/MnO₂ are 87.4, 62.7, 60.5, 57.4, and 54.4 F g⁻¹ at scan rate ranging from 5 to 100 mV/s, respectively. All CV curves show the similar shapes, further suggesting the excellent reversibility and ultrafast charging capability of the PEDOT:PSS/MnO₂ films with 50 wt.% MnO₂. Compared with pure PEDOT:PSS electrode, the evident redox peaks for composite electrodes indicate that the enhanced capacitance of the PEDOT:PSS/MnO₂ electrodes mainly come from the faradaic redox reaction, which results in a large active area. This is attributed to the active MnO₂ NPs embedded in PEDOT:PSS network. Meanwhile, the good electron transport property of PEDOT:PSS effectively promote surface redox reactions of MnO₂ with electro-absorption of cations (Na⁺ and H⁺) and intercalation-de-intercalation processes of the protons according to the following reaction:[36]



The anodic and cathodic peaks shift to higher and lower potentials with the increasing scan rate, respectively, which is related to performance of pseudocapacitors owing to the quasi-reversible characteristic of the redox reactions.[37] Eventually, it can be found that the PEDOT:PSS/MnO₂ film with 50 wt.% MnO₂ does not only present good flexibility and free-standing property, but also shows enhanced capacitance performance compared to pure PEDOT:PSS. It can be seen from Table 1 that a number of different PEDOT-based materials for supercapacitors have been reported so far. Traditional PEDOT-based materials present poor flexibility and free-standing property. In comparison, the PEDOT:PSS/MnO₂ films show better performance for supercapacitor with promising application in wearable electron devices.

Table 1. Performance of PEDOT-based material for supercapacitor.

Composite material	Specific capacitance (F/g)	Flexibility	Free-standing	Ref.
PEDOT/MnO ₂	169	-	No	[12]
PVA-MnO ₂ /PEDOT	107.22	-	No	[38]
PVA-GO/PEDOT	94.73	-	No	[38]
PEDOT/GO	73.3	-	No	[39]
PBEDTH	40.8	Flexibility	Free standing	[40]

4. CONCLUSION

In summary, α -MnO₂ NPs were prepared by a simple and environmental friendly method and used to enhance the capacitance properties of PEDOT:PSS films. The flexible free-standing PEDOT:PSS/MnO₂ composite films were fabricated by direct dilution-filtration. The electrical conductivity of the PEDOT:PSS/MnO₂ composite electrodes was greatly enhanced by dilution-filtration with ethanol. The MnO₂ NPs contents in PEDOT:PSS have positive effect on the electrochemical capacitance performance of composite films. Meanwhile, the PEDOT:PSS promoted the good film-forming property and achieved high electron transport property. When the MnO₂ NPs content was 50 wt.%, the composite electrode achieved the maximum capacitance performance with good flexibility and free-standing property. This work on the fabrication of free-standing electrodes proposes a new

strategy and provides corresponding reference for the development of flexible wearable energy devices in the future.

ACKNOWLEDGEMENTS

The authors would like to thank the financial support of National Natural Science Foundation of China (51762018, 51463008, 51572117, and 11564015), the Innovation Driven "5511" Project of Jiangxi Province (20165BCB8016).

References

1. P. Tang, L. Han and L. Zhang, *ACS Appl. Mater. Interfaces*, 6 (2014) 10506.
2. G. Wang, L. Zhang and J. Zhang, *Chem. Soc. Rev.*, 41 (2012) 797.
3. Q. Zhou, D. Zhu, X. Ma, D. Mo, F. Jiang, J. Xu and W. Zhou, *Electrochim. Acta*, 212 (2016) 662.
4. J. Xu, Y. Sun, M. Lu, L. Wang, J. Zhang, J. Qian and X. Liu, *Chem. Eng. J.*, 334 (2018) 1466.
5. H. Jia, Y. Cai, J. Lin, H. Liang, J. Qi, J. Cao, J. Feng and W. Fei, *Adv. Sci.*, 5 (2018) 1700887.
6. Z.-H. Huang, Y. Song, D.-Y. Feng, Z. Sun, X. Sun and X.-X. Liu, *ACS Nano*, 12 (2018) 3557.
7. Z. Li, G. Ma, R. Ge, F. Qin, X. Dong, W. Meng, T. Liu, J. Tong, F. Jiang, Y. Zhou, K. Li, X. Min, K. Huo, and Y. Zhou, *Angew. Chem. Int. Ed.*, 128 (2016) 991.
8. L. Hu, M. Pasta, F. La Mantia, L. Cui, S. Jeong, H. D. Deshazer, J. W. Choi, S. M. Han and Y. Cui, *Nano Lett.*, 10 (2010) 708.
9. Z. Lv, Y. Luo, Y. Tang, J. Wei, Z. Zhu, X. Zhou, W. Li, Y. Zeng, W. Zhang, Y. Zhang, D. Qi, S. Pan, X. J. Loh and X. Chen, *Adv. Mater.*, 30 (2018) 1704531.
10. M. Zhang, Q. Zhou, J. Chen, X. Yu, L. Huang, Y. Li, C. Li and G. Shi, *Energy Environ. Sci.*, 9 (2016) 2005.
11. R. Qi, J. Nie, M. Liu, M. Xia and X. Lu, *Nanoscale*, 10 (2018) 7719.
12. A. O. Nizhegorodova, S. N. Eliseeva, E. G. Tolstopjatova, G. G. Láng, D. Zalka, M. Ujvári and V. V. Kondratiev, *J. Solid State Electr.*, 22 (2018) 2357.
13. Y. Chang, W. Zhou, J. Wu, G. Ye, Q. Zhou, D. Li, D. Zhu, T. Li, G. Nie, Y. Du and J. Xu, *Electrochim. Acta*, 283 (2018) 744.
14. Z. Su, C. Yang, C. Xu, H. Wu, Z. Zhang, T. Liu, C. Zhang, Q. Yang, B. Li and F. Kang, *J. Mater. Chem. A*, 1 (2013) 12432.
15. H. Zhou, G. Han, Y. Chang, D. Fu and Y. Xiao, *J. Power Sources*, 2015, 274, 229.
16. C. Zhang, T. M. Higgins, S.-H. Park, S. E. O'Brien, D. Long, J. N. Coleman and V. Nicolosi, *Nano Energy*, 28 (2016) 495.
17. Y. Chen, B. Xu, J. Wen, J. Gong, T. Hua, C.-W. Kan and J. Deng, *Small*, 14 (2018) 1704373.
18. J. Xiong, F. Jiang, W. Zhou, C. Liu and J. Xu, *RSC Adv.*, 5 (2015) 60708.
19. Y. Zhu, N. Li, T. Lv, Y. Yao, H. Peng, J. Shi, S. Cao and T. Chen, *J. Mater. Chem. A*, 6 (2018) 941.
20. J. Luo, Z. Zheng, A. Kumamoto, W. I. Unah, S. Yan, Y. H. Ikuhara, X. Xiang, X. Zu and W. Zhou, *Chem. Comm.*, 54 (2018) 794.
21. S. Zheng, Z.-S. Wu, S. Wang, H. Xiao, F. Zhou, C. Sun, X. Bao and H.-M. Cheng, *Energy Storage Mater.*, 6 (2017) 70.
22. W. Chen, D. Gui and J. Liu, *Electrochim. Acta*, 222 (2016) 1424.
23. G. P. Ojha, B. Pant, S.-J. Park, M. Park and H.-Y. Kim, *J. Colloid Interfaces Sci.*, 494 (2017) 338.
24. Y. Zhang, H. Xuan, Y. Xu, B. Guo, H. Li, L. Kang, P. Han, D. Wang and Y. Du, *Electrochim. Acta*, 206 (2016) 278.
25. S. Zhu, L. Li, J. Liu, H. Wang, T. Wang, Y. Zhang, L. Zhang, R. S. Ruoff and F. Dong, *ACS Nano*, 12 (2018) 1033.

26. R. Peng, N. Wu, Y. Zheng, Y. Huang, Y. Luo, P. Yu and L. Zhuang, *ACS Appl. Mater. Interfaces*, 8 (2016) 8474.
27. W. Dang, C. Dong, Z. Zhang, G. Chen, Y. Wang and H. Guan, *Electrochim. Acta*, 217 (2016) 16.
28. Y. Ren, Q. Xu, J. Zhang, H. Yang, B. Wang, D. Yang, J. Hu and Z. Liu, *ACS Appl. Mater. Interfaces*, 6 (2014) 9689.
29. J. W. Lee, A. S. Hall, J.-D. Kim and T. E. Mallouk, *Chem. Mater.*, 24 (2012) 1158.
30. Z. Li, Y. An, Z. Hu, N. An, Y. Zhang, B. Guo, Z. Zhang, Y. Yang and H. Wu, *J. Mater. Chem. A*, 4 (2016) 10618.
31. T. Zhu, S. J. Zheng, Y. G. Chen, J. Luo, H. B. Guo and Y. E. Chen, *J. Mater. Sci.*, 49 (2014) 6118.
32. Y. Xia, K. Sun and J. Ouyang, *Adv. Mater.*, 24 (2012) 2436.
33. G. H. Kim, L. Shao, K. Zhang and K. P. Pipe, *Nat. Mater.*, 12 (2013) 719.
34. X.-X. Li, X.-H. Deng, Q.-J. Li, S. Huang, K. Xiao, Z.-Q. Liu and Y. Tong, *Electrochim. Acta*, 264 (2018) 46.
35. L. Ni, Z. Wu, G. Zhao, C. Sun, C. Zhou, X. Gong and G. Diao, *Small*, 13 (2017) 1603466.
36. H. Pang, S. Wang, G. Li, Y. Ma, J. Li, X. Li, L. Zhang, J. Zhang and H. Zheng, *J. Mater. Chem. A*, 1 (2013) 5053.
37. T. Yao, Y. Li, D. Liu, Y. Gu, S. Qin, X. Guo, H. Guo, Y. Ding, Q. Liu, Q. Chen, J. Li and D. He, *J. Power Sources*, 379 (2018) 167.
38. M. Abdah, N. Rahman and Y. Sulaiman, *Electrochim. Acta*, 259 (2018) 466.
39. N. Azman, H. Lim, M. Mamat and Y. Sulaiman, *Energies*, 11 (2018) 1510.
40. G. Ye, J. Xu, X. Ma, Q. Zhou, D. Li, Y. Zuo, L. Lv, W. Zhou and X. Duan, *Electrochim. Acta*, 224 (2017) 125.